

## Free paper session 7: New materials I

### KL7.1

#### **(Supra-)molecular strategies towards printable hydrogels**

Jürgen Groll

*University Hospital Würzburg, Würzburg, Germany*

Biofabrication originated rather from the (bio-)engineering community that is familiar with printing technologies and did not evolve from chemistry or materials science. Accordingly the field has for long worked with the most established hydrogel systems available in quantities that are necessary for the processes. Hence the vast majority of literature studies use (modified or supplemented) alginate and gelatine as base material. Although this has allowed achieving some remarkable successes it has become more and more evident that the lack of variety in printable hydrogel systems is one major drawback for the complete field<sup>1 2</sup>.

Hence the scope of this lecture will not be to recapitulate the different established printing methods and summarize the hydrogels used for printing so far. The main objective will be to complement this information with an introduction into the most important rheological aspects of printing and an overview of possibilities to create tailored molecular building blocks for printable hydrogels. This overview comprises existing strategies in related research fields such as supramolecular chemistry for self-assembly strategies or biotechnological approaches for bioinspired building blocks. The aim is to deliver a comprehensive set of information to be used as a toolbox along with a basic set of fundamental design criteria for the rational development of novel strategies towards versatile bioinks.

Literature

- 1) Malda J. et al. *Adv. Mater.* 2013 25 5011-5028.
- 2) Skardal A. et al. *Ann. Biomed. Eng.* 2014 43 730-746.



## F7.1

### **3D Bioprinting of human chondrocytes and induced pluripotent stem cells in nanocellulose bioink for customized cartilage tissue engineering**

Daniel Hägg, Theodoros Kalogeropoulos, Duong Nguyen, Annika Enejder, Paul Gatenholm, Stina Simonsson

*Chalmers University of Technology, Göteborg, Sweden*

**Introduction:** The ability to create 3D cartilage tissue on demand would enable scientific and technological advances in tissue engineering and regenerative medicine as well as in basic research and drug screening. Using 3D bioprinting customized grafts can be engineered using bottom-up technology that precisely fits the site of injury such as in patients suffering from osteoarthritis.

Nanocellulose is an emerging biomaterial that has similar properties to collagen and thus can mimic native extracellular matrix compounds. We have previously used nanocellulose to develop artificial blood vessels and scaffolds for cartilage tissue engineering. In this study we aim to use 3D bioprinting to develop a method for engineering cartilage tissue in customized shapes and form.

**Materials and methods:** In this study a bioink of nanocellulose and alginate was developed for 3D bioprinting. Initially confocal microscopy was used to verify that iPS cells could adhere to 3D structures of the bioink. Bioinks of different fractions of nanocellulose and alginate were then prepared and used to encapsulate human iPS cells and chondrocytes either separately or together. Different patterns were printed and the viability of the cells was evaluated after printing. Proliferation was analyzed using MTS. Cell distribution was analyzed with non-linear microscopy and chondrogenic differentiation was analyzed using immunohistochemistry.

**Results:** The initial experiments verified that the iPS cells could attach and grow on the bioink material verified using immunofluorescence for Oct4 and dapi. After bioprinting with cells encapsulated in the bioink viable cells were found after up to 35 days. MTS revealed a 3-fold increase in metabolic activity after four days indicating a suitable environment for growing cells. Using a lower concentration of nanocellulose yielded a higher number of cells within the printed constructs whereas a higher amount of nanocellulose yielded more stable constructs. The iPS cells and the chondrocytes were thereafter printed in separate strands in an overlapping grid structure. The production of GAGs was increased in the intersections indicating a crosstalk between chondrocytes and iPS cells.

**Discussion:** We conclude that the developed bioink is well suited for bioprinting with iPS cells and chondrocytes sustaining cell viability over time. By controlling the positioning of the cells in a 3D distribution the chondrogenic differentiation of iPS cells can be enhanced through cell-cell crosstalk.

#### *Acknowledgements:*

This research was supported by Chalmers Materials Area of Advance and Vinnova and Eureka program; EUROSTARS E18355 CELLINK.



## F7.2

### Bioprinting of mechanically strong cell-laden fibres

Jing Yang, Ahmed Aied, Kevin Shakesheff, Pritesh Mistry  
*University of Nottingham, Nottingham, United Kingdom*

**Aim:** Fibre based strategy is attractive for creating 3D complex hierarchical human tissues in vitro because they mimic fibrous human tissues such as tendon ligament and muscle. These fibres need to offer an extra cellular matrix-like environment for the interaction with cells and also to be mechanically strong so it is robust during handling and can bear in vivo loading after implantation. Here we report a study on 3D printing of fibres which are mechanically robust as well as have chemistry suitable for cell survival and function.

**Method:** In this study a modified commercial 3D printer was used to print the fibres which are mechanical strong and encapsulate cells. Fibres were made from a composite material that exhibited superior biological and mechanical properties compared to its individual components. These fibres were characterised by mechanical testing; cell viability and function within these fibres were also characterised. These fibres were printed into 3D structures.

**Results:** The composite material showed a 3 fold increase in ultimate tensile strength compared to its individual components. The failure strain was also significantly increased. The cells that are encapsulated in the material showed good viability and proliferation which suggested that the material allowed sufficient nutrient and oxygen transport into the encapsulated cells. The material could be extruded during 3D printing to form different 3D structures such as tubes and meshes.

**Conclusion:** Fibres with good biological and mechanical properties have been made and laid into different structures using 3D printing. These fibres can potentially be used in load bearing applications.



*Micrograph of a printed fibre with encapsulated cells.*

### F7.3

#### **3D plotting of cell-laden alginate/methylcellulose blends – a simple and versatile method for diverse bioprinting approaches**

Anja Lode, Kathleen Schütz, Sophie Brüggemeier, Michael Gelinsky  
*Technische Universität Dresden Faculty of Medicine Centre for Translational Bone Joint and Soft Tissue Research, Dresden, Germany*

The challenge of biofabrication is to generate 3D constructs with high shape fidelity but also with cell-friendly properties. The aim of our group was to develop an alginate-based material which combines suitable features for both accurate deposition and cell embedding by using a simple strategy. During fabrication the biopolymer concentration was temporarily increased by addition of methylcellulose (MC) to low concentrated alginate. The enhanced viscosity strongly improved the printing properties enabling the generation of 3D structures with dimensions in the centimeter-range. After plotting MC did not contribute to the Ca<sup>2+</sup>-induced gelation and was released from the scaffolds during following cultivation. The resulting constructs were characterized by high stability and an enhanced microporosity caused by the transient presence of MC. The suitability of the alginate/MC blend as cell carrier was evaluated by incorporation of mesenchymal stem cells (hMSC) during scaffold fabrication: the cells survived the plotting process (Fig. 1A) and viable cells were also detected after cultivation for 21 days; differentiation potential of the embedded hMSC was proven for the adipogenic lineage.

By definition biofabrication has potential applications also beyond the traditional medically oriented ones [1]. By using the unicellular microalga *Chlamydomonas reinhardtii* as model organism we demonstrated that bioprinting can be extended to cells originating from the plant kingdom ('Green Bioprinting'). The algae grew within the hydrogel matrix under illumination (Fig. 1B); photosynthetic activity was evidenced by measurement of oxygen release [2]. The hydrogel blend allows the fabrication of cell-laden constructs with tailored architecture for applications in medicine and biotechnology.

Funding by the Saxon Ministry for Higher Education and Arts and the Excellence Initiative by the German Federal and State Governments (Institutional Strategy measure "support the best") is acknowledged.

[1] Mironov *Biofabrication* 2009 1 022001

[2] Lode *Eng Life Sci* 2015 15 177



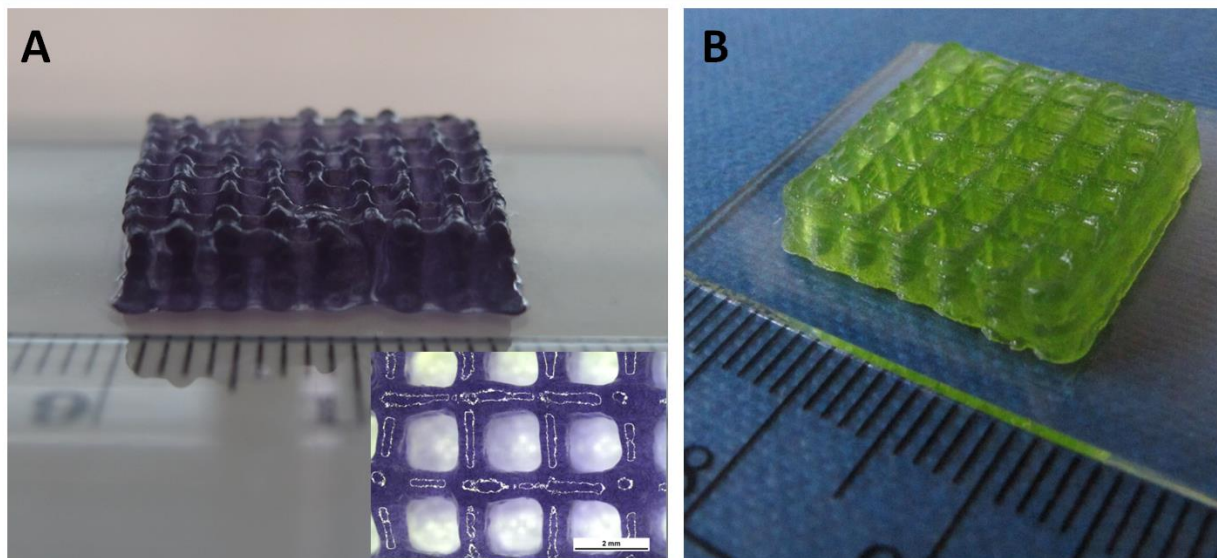


*Fig. 1: Algininate/MC scaffolds with A) embedded hMSC (d1, MTT staining of viable cells) and B) embedded green microalgae (d6)*



#### F7.4

##### Cell encapsulation for bio-ink formulation

Ricardo Ribeiro, Ana Ferreira Duarte, Matthew Benning, Deepali Pal, David Jamieson, Kenneth Samora Rankin, Kenneth Dalgarno  
*Newcastle University – School of Mechanical and Systems Engineering, Newcastle Upon Tyne, United Kingdom*

**Aim:** Single cell encapsulation with a semi-permeable biodegradable shell is an attractive procedure for a range of biomedical applications<sup>1</sup>. Nozzle clogging is one limitation of inkjet bioprinting which makes the process unreliable<sup>2</sup>. This work explored the use of poly-L-lysine (PLL) to encapsulate single osteosarcoma cells (U2OS cells) evaluating the effect of different PLL concentrations on the viability and morphology of the cells. **Methods:** Single U2OS cells were encapsulated into PLL shells using three concentrations: 100, 50 and 10 µg/ml. Cell viability was evaluated by MTT and Live-Dead assays, fluorescence-activated cell sorting (FACS) and ImageStream, with the latter two techniques also used to assess the encapsulation efficiency. The mechanism of capsule release was studied using transmission electron microscopy (TEM) and cell morphology by fluorescence and confocal microscopy. Coated and non-coated cells were printed using an inkjet bioprinter and its reliability assessed by printing droplets at 10-minute intervals over a one hour period and subsequently counting cells. **Results:** Over 99% of cells were encapsulated. A viability increase with polymer concentration decrease was demonstrated, with 94% healthy cells with the lowest concentration immediately after encapsulation. At higher concentrations cells were found to still be encapsulated 4 hours after coating and undergoing necrosis. The cytotoxic effect of the higher polymer concentrations was confirmed by TEM, where highly vacuolated cells and polymer uptake was observed. A reliable bio-ink was obtained with a consistent print yield over the period. Printed cells were viable. **Conclusions:** Cell encapsulation can be used as a mechanism to stabilise bio-inks in order to achieve consistent printing yields over extended time periods of up to an hour. The mechanism of degradation involves both dissolution of the shell and ingestion of the polymer by the cells, and for encapsulation using a 10 µg/ml concentration of PLL occurs over a timeframe of a few days.

##### *References:*

1 Germain (2006) *Biosensors and Bioelectronics* 21:1566-73; 2 Murphy (2014) *Nature Biotechnology* 32: 773-785.

##### *Acknowledgements:*

The research reported in this paper has been partly funded through MeDe Innovation (the EPSRC Centre for Innovative Manufacture in Medical Devices), the EPSRC Centre for Innovative Manufacture in Additive Manufacture, the Arthritis Research UK Tissue Engineering Centre, and a Newcastle University Doctoral Studentship. Trevor Booth and Kathryn White are acknowledged for the support on imaging acquisition.



**F7.5**

**Biodegradable thermoplastic elastomers for use in biofabrication**

Aysun Güney, Jos Malda, Wouter Dhert, Dirk Grijpma  
 University of Twente, Enschede, Netherlands

**Aim:** Extrusion-based additive manufacturing processes are of interest in preparing designed implants for biomedical applications<sup>1</sup>. However the number of biodegradable polymers available for biofabrication is limited. Particularly interesting are block-copolymers as their physical properties can readily be tuned by variation of the nature and length of the respective blocks<sup>2</sup>. Here we prepared triblock copolymers based on 1,3-trimethylene carbonate (TMC) and  $\epsilon$ -caprolactone (CL) by different methods and evaluated their potential as melt processable thermoplastic elastomeric biomaterials.

**Methods:** PCL-b-PTMC-b-PCL triblock copolymers that combine a soft PTMC block (20 kDa) and hard crystallisable PCL (10 kDa) blocks were synthesized by different methods using stannous octoate Sn(Oct)<sub>2</sub> and diphenyl phosphate (DPP) as catalysts: 1) A dihydroxyl-terminated PTMC polymer was prepared by ring opening polymerization (ROP) of TMC (FORYOU Company) and used to initiate the ROP of CL. 2) The dihydroxyl-terminated PTMC was reacted with monofunctional isocyanate-terminated PCL to polyurethane block-copolymers. The polymers were characterized by GPC and DSC.

**Results:** The molecular weight (MW) of the polymers are somewhat lower than intended. When PTMC is used to initiate the ROP of CL the use of DPP leads to higher MW of the copolymer than the use of Sn(Oct)<sub>2</sub>. In the polyurethane formation Sn(Oct)<sub>2</sub> seems to be most effective. Higher MW copolymers are formed although the melting temperatures of the PCL are lower. These polyurethanes now show melting points approximately 150 to 160°C. In general the use of DPP resulted in lower polydispersity indices than when Sn(Oct)<sub>2</sub> is used.

**Conclusions:** When high molecular weight triblock copolymers are prepared by sequential monomer addition use of DPP is preferred. On the other hand when copolymers containing urethane bonds are to be formed Sn(Oct)<sub>2</sub> is the more effective catalyst.

*References:*

- 1) Dababneh et al. J. Manuf. Sci. Eng. 2014 136 061016-11.
- 2) Park et al. Polymer 2003 44 6725.

| Method                      | Catalyst             | Intended Polymer  | M <sub>n</sub> (GPC)<br>(kg/mol) | PDI | T <sub>g1</sub> (°C) | T <sub>g2</sub> (°C) | T <sub>m1</sub><br>(°C) | T <sub>m2</sub><br>(°C) |
|-----------------------------|----------------------|---|----------------------------------|-----|----------------------|----------------------|-------------------------|-------------------------|
| Sequential Monomer Addition | Sn(Oct) <sub>2</sub> | PTMC <sub>20k</sub>   | 17.4                             | 1.8 | -                    | -19                  | -                       | -                       |
|                             |                      | PCL <sub>10k</sub> -PTMC <sub>20k</sub> -PCL <sub>10k</sub> | 30.1                             | 1.8 | -58                  | -20                  | 48                      | -                       |
|                             | DPP                  | PTMC <sub>20k</sub>   | 16.3                             | 1.1 | -                    | -19                  | -                       | -                       |
|                             |                      | PCL <sub>10k</sub> -PTMC <sub>20k</sub> -PCL <sub>10k</sub> | 35.1                             | 1.2 | -60                  | -21                  | 51                      | -                       |
| Polyurethane Formation      | Sn(Oct) <sub>2</sub> | PTMC <sub>20k</sub>   | 17.4                             | 1.8 | -                    | -19                  | -                       | -                       |
|                             |                      | PCL <sub>10k</sub> -PTMC <sub>20k</sub> -PCL <sub>10k</sub> | 27.9                             | 1.4 | -61                  | -20                  | 53                      | 152                     |
|                             | DPP                  | PTMC <sub>20k</sub>   | 16.3                             | 1.1 | -                    | -19                  | -                       | -                       |
|                             |                      | PCL <sub>10k</sub> -PTMC <sub>20k</sub> -PCL <sub>10k</sub> | 20.2                             | 1.5 | -57                  | -20                  | 60                      | 161                     |

